

## College of Engineering



Drexel E-Repository and Archive (iDEA)

<http://idea.library.drexel.edu/>

Drexel University Libraries

[www.library.drexel.edu](http://www.library.drexel.edu)

The following item is made available as a courtesy to scholars by the author(s) and Drexel University Library and may contain materials and content, including computer code and tags, artwork, text, graphics, images, and illustrations (Material) which may be protected by copyright law. Unless otherwise noted, the Material is made available for non profit and educational purposes, such as research, teaching and private study. For these limited purposes, you may reproduce (print, download or make copies) the Material without prior permission. All copies must include any copyright notice originally included with the Material. **You must seek permission from the authors or copyright owners for all uses that are not allowed by fair use and other provisions of the U.S. Copyright Law.** The responsibility for making an independent legal assessment and securing any necessary permission rests with persons desiring to reproduce or use the Material.

Please direct questions to [archives@drexel.edu](mailto:archives@drexel.edu)

## Numerical Derivative Analysis of Load-Displacement Curves in Depth-Sensing Indentation

Tom Juliano<sup>1</sup>, Vladislav Domnich<sup>1</sup>, Tom Buchheit<sup>2</sup>, and Yury Gogotsi<sup>1</sup>

<sup>1</sup>*Department of Materials Science and Engineering Drexel University, Philadelphia, PA 19104, USA*

<sup>2</sup>*Department of Microsystems, Materials, Tribology and Technology - Sandia National Laboratories, Albuquerque, NM 87185, USA*

### ABSTRACT

The use of load-displacement derivative behavior and power-law curve fitting is applied to find the location of events for a number of different materials during depth-sensing indentation. Load-displacement curves for Berkovich indentations on fused silica, fullerene thin film on sapphire, CdTe thin film on silicon, single crystal silicon, carbide derived carbon, and a polymethylmethacrylate/hydroxyapatite (PMMA/HA) particle composite are examined. The analysis is applied to quantify the location of different events that occur during material loading and unloading.

### INTRODUCTION

Depth-sensing indentation is a technique used to characterize local mechanical properties of small volumes for many types of solid materials and thin films. Load and displacement data is collected throughout a typical indentation experiment and standard techniques such as the Oliver and Pharr method [1] are used to extract hardness and modulus properties for isotropic solids. Recent improvements in load-displacement data analysis have led to accurate property measurements on thin films [2]. In such cases, the Oliver and Pharr method must be modified to allow for substrate effects.

For many materials, discrete phenomena such as phase transformation, dislocation nucleation, or cracking take place during indentation testing, showing up as transient events in the resultant load-displacement curve. Sapphire has been shown to exhibit a significant “pop-in” displacement feature in its loading curve, due to dislocation nucleation, when spherical indenter tips are used [3]. For silicon indentation with spherical tools, the pop-in feature upon loading, which is proposed to be due to phase transformation from cubic-diamond Si-I to  $\beta$ -tin Si-II, has been found [4,5]. In the silicon unloading curve, elbowing (continual decrease in slope of unloading curve) and pop-out features have been observed for both sharp and spherical tools [5,6]. Both events were shown to be due to different phase transformations [6]. Phase-transformation-induced features in unloading curves of germanium and some other materials have also been found [7]. The presence or nature of a particular event shape can depend on crystal orientation, loading or unloading rate, number of loading cycles, indentation depth, or indenter geometry. However, these discrete events cannot be analyzed by conventional techniques that require load-displacement data to form continuous curves during loading and unloading portions of the experiment. For this reason, it is necessary to develop quantitative methods to determine the point where the event, whatever mechanism it is due to, begins.

Hainsworth *et al.* [8] illustrated that for geometrically self-similar indenter tips, such as Berkovich, conical or pyramidal, the indentation load  $P$  and the indentation depth  $h$  were experimentally related for most materials during loading by the expression

$$P = Kh^2 \quad (1)$$

where  $K$  is a material-dependent constant. This was confirmed for a number of metals and ceramics [9]. It was demonstrated that for some materials, however, better fits can be obtained when the power of  $h$  is less than 2, namely

$$P = Kh^n \quad (2)$$

where  $n$  falls somewhere between about 1.5 and 2 [8]. This equation has been shown to be true for both soft [10] and hard [11,12] coatings deposited on hard substrates, with the slope of  $P$  vs.  $h^n$  changing when substrate effects or cracks appear. More recently, Malzbender and de With have incorporated more dependencies to see the point at which fracture of coatings begins [13]. They have used plots of  $P/h^2$  vs.  $h^2$  and  $\partial P/\partial(h^2)$  vs.  $h^2$  for Berkovich indentation to more clearly see these event points, based on the knowledge that  $K$  in Eq. (1) will change when hardness or modulus properties change. However, derivative calculation methods seemed to not be very precise and produced somewhat ambiguous event locations.

During unloading, the Oliver-Pharr method relates the load and displacement as

$$P = \alpha(h - h_f)^m \quad (3)$$

where  $\alpha$  is a curve fitting parameter,  $h_f$  is the final residual indentation depth, and  $m$  is a curve fitting parameter ranging from 1 to 2 [1]. Finite element simulations of indentation experiments have been performed and it was found that Eq. (3) closely describes the simulated unloading curve, as well as what has been found during experimentation [14]. The exponent  $m$  will not be a constant when transient events appear in the unloading curves, and to the knowledge of the authors, the usefulness of derivative behavior during unloading has never been addressed.

It follows that for a given set of data points, it is easier for the eye to detect changes in the deviation of an approximately straight line than from a parabolic-type function. Therefore, taking numerical derivatives of Eqs. (2) and (3) as functions of  $h$  is especially useful when  $n$  in Eq. (2) and  $m$  in Eq. (3) are close to two. This article describes several examples illustrating the usefulness of numerical derivative behavior for load vs. displacement data to identify the location of discrete transient events that occur during indentation testing. Fused silica results are first presented as baseline material behavior. Then, fullerene thin film on sapphire, CdTe thin film on silicon, single crystal silicon, carbide derived carbon (CDC), and a polymethylmethacrylate/hydroxyapatite (PMMA/HA) particle matrix behavior are compared with this baseline behavior. Load-displacement and derivative behavior for transient events during loading, kink pop-out, elbowing behavior, and sharp unloading curve bending for this material set will be examined. This technique can be applied to materials that exhibit phase transformation, cracking, delamination, dislocation nucleation, or any other type of discrete phenomenon that can be detected from a load-displacement curve generated by a depth-sensing indentation experiment.

**Table 1:** Summary of materials used in this study, events, loading conditions, hardness, and modulus values. For hardness and modulus values, commas denote respective components of the material system. For example, “0.22, 21” refers to hardness values of C<sub>60</sub> thin films and sapphire, respectively.

Material	Event	Max Applied Load (mN)	Load/Unload Time (s)	Hardness (GPa)	Modulus (GPa)
Fused Silica	None	50	30/30	9.5	72
C60 Thin Film/ Sapphire Substr.	Transient Loading Event	50	30/30	0.22, 21	MPa Range, 335
CdTe Thin Film/ Silicon (111) Substr.	Transient Loading Event	100	30/30	0.6, 11.3	3.7, 170
Silicon (111)	Kink Popout	100	30/15	11.3	170
Silicon (111)	Elbowing	40	30/15	11.3	170
Soft CDC	Elbowing	20	30/30	1.5	12
Hard CDC	Sharp Unloading Curve Bending	50	30/30	14	340
PMMA/HA Partide Matrix	Sharp Unloading Curve Bending	200	30/30	MPa Range, 6.5	1, 125

## MATERIALS AND EXPERIMENTAL PROCEDURE

An MTS Nano Indenter XP (MTS Systems, Tennessee) was used to obtain all indentation load-displacement curves in ambient conditions. A diamond Berkovich indenter with an effective radius of about 100 nm was used to make the indentations. Indentation load-displacement curves were gathered on fused silica, ~4 μm thick C<sub>60</sub> film deposited on a sapphire substrate, a 13 μm thick CdTe film deposited on a silicon wafer, single-crystal (111) silicon, CDC ~20 μm thick, and HA particles in PMMA with an average particle diameter of 20 μm. At least ten indentation tests were performed on each material. The materials were chosen because they display a variety of transient events seen in both loading and unloading curves, which are presented in the results and discussion section. In all cases, the data collection rate was set at 5 Hz. Load control was used so that successive data points are in constant load increments as compared to constant displacement increments. The maximum applied load ranged from 20 to 500 mN, depending on the sample. In most cases, the material was loaded over 30 seconds, the maximum load was held for 30 seconds and completely unloaded over 30 seconds. Some single-crystal silicon indentations were unloaded over a shorter time period to produce certain curve shapes. A summary of all material properties, loading conditions, and transient events considered in this study is given in Table 1.

The derivative behavior was numerically extracted from the loading and unloading portions of the load-displacement curves. The numerical first derivative at a depth  $h_x$  was taken to be the slope of the least-squares fit between load-displacement data points and given as

$$\left(\frac{dP}{dh}\right)_{h_x} = \frac{y \begin{pmatrix} P_{x+\frac{y-1}{2}} \\ \sum Ph \\ P_{x-\frac{y-1}{2}} \end{pmatrix} \begin{pmatrix} h_{x+\frac{y-1}{2}} \\ \sum h \\ h_{x-\frac{y-1}{2}} \end{pmatrix} - \begin{pmatrix} h_{x+\frac{y-1}{2}} \\ \sum h \\ h_{x-\frac{y-1}{2}} \end{pmatrix} \begin{pmatrix} P_{x+\frac{y-1}{2}} \\ \sum P \\ P_{x-\frac{y-1}{2}} \end{pmatrix}}{y \begin{pmatrix} h_{x+\frac{y-1}{2}} \\ \sum (h^2) \\ h_{x-\frac{y-1}{2}} \end{pmatrix} - \begin{pmatrix} h_{x+\frac{y-1}{2}} \\ \sum h \\ h_{x-\frac{y-1}{2}} \end{pmatrix}} \quad (4)$$

where  $y$  is a positive odd integer number of data points considered and  $x$  refers to the data point (element) number in the column output. It was found that five points produced the best numerical derivatives. If  $y$  was three, there was significantly more noise present in the resulting derivative curves. If  $y$  was set to seven or greater, the event locations were not as pronounced. The best values for  $y$  will depend on data point collection frequency, and the most effective values should be determined experimentally. It was also found useful to take the derivative at  $h_x$  to be

$$\left(\frac{dP}{dh}\right)_{h_x} = \frac{P_{x+\left(\frac{y-1}{2}\right)} - P_{x-\left(\frac{y-1}{2}\right)}}{h_{x+\left(\frac{y-1}{2}\right)} - h_{x-\left(\frac{y-1}{2}\right)}} \quad (5)$$

to make computation easier, however there is a greater amount of noise present in the resulting plots for a given value of  $y$ . Second derivatives were computed based on Eq. (5), but no additional information could be obtained for the materials in study.

## RESULTS AND DISCUSSION

### I. Standard Behavior

Fused silica is frequently used as a calibration standard for depth-sensing indentation testing. In this article it provides a standard for derivative behavior. A typical load-displacement curve for fused silica is shown in Fig. 1(a). The resultant derivative behavior is presented for the respective loading and unloading segments in Figs. 1(b) and 1(c). If Eq. (1) accurately predicts the indentation loading response, then the derivative behavior during loading will be linear. If the exponent  $n$  in Eq. (2) is less than 2, then the derivative response will have downward concavity. Likewise, if  $n$  is greater than 2, the derivative response will have upward concavity. It can be seen in Fig. 1(b) that Eq. (1) accurately predicts the loading behavior for fused silica since derivative behavior is linear. Consistent with Reference 14, the unloading curve for silica was best fit to Eq. (3) when the exponent  $m$  is about 1.25. Therefore, the derivative behavior displays downward concavity because  $m$  is less than two.

Figs. 1(b) and 1(c) show increasing scatter in the derivative behavior toward the end of the loading segment and toward the beginning of the unloading segment. This is due to how the data points are collected in the load-controlled mode and consideration of the numerical derivative segment length. Fig. 2 shows schematically the length of the data segment for the beginning (a) and final part of loading (b). It can be seen that although a constant time or load interval is present between data points, the average derivative segment length may vary greatly as the slope of the curve increases at greater indentation depths. During unloading, the reverse is true and the data intervals become longer as the experiment progresses to shallower indentation depth. Consequently, shorter numerical derivative lengths are seen to generate more noise in the calculated data. As such, it can be seen in Fig. 1 that the steepest section of the fused silica load-displacement curve yields the noisiest behavior, which is at the beginning of the unloading segment.

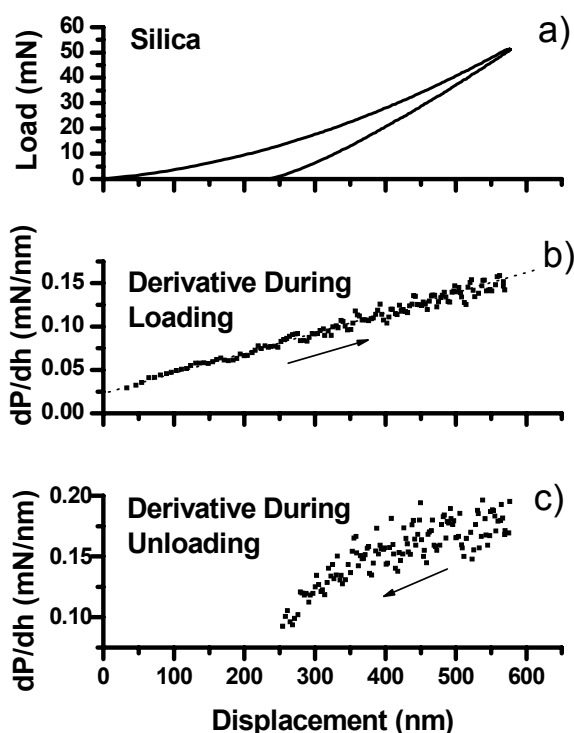


**Figure 1:** Load-displacement curve for fused silica (a), and first derivative behavior during loading (b) and unloading (c). No events are observed in the curves, and the sudden changes are due to noise in the data. The dashed line shows a linear fit.

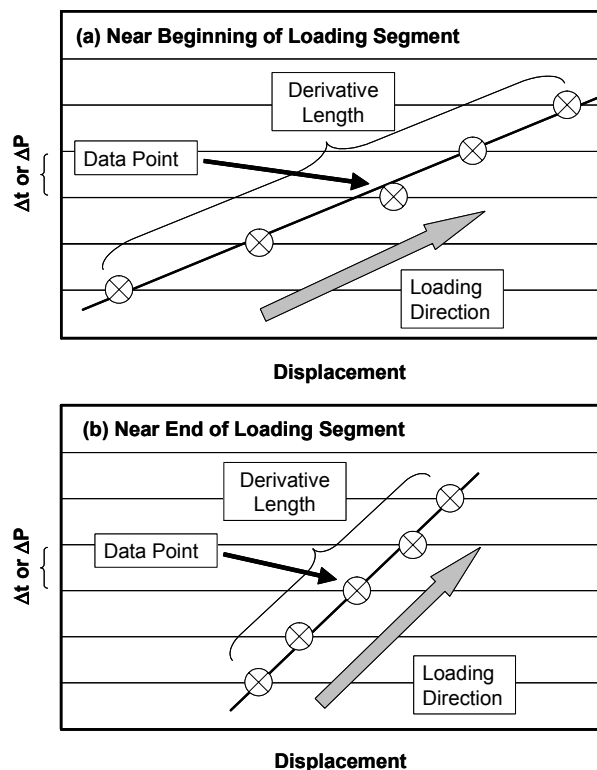


**Figure 2:** Schematic derivative segment lengths for the beginning (a) and end (b) of the loading segment.

## II. Transient Events During Loading

Two material systems, each composed of a soft thin film on a hard substrate, exhibited transient behavior during indentation loading. The first is the fullerene film on sapphire. Fullerene thin films are very soft relative to sapphire with their hardness reported to be about 0.22 GPa [15] (Table 1). Load-displacement and derivative behavior is given in Fig. 3. The selected load-displacement curve (Fig. 3(a)) shows a subtle transient event near a displacement of 1500 nm. The derivative analysis (Fig. 3(b)) reveals typical behavior ( $P \propto h^2$ ) to 1500 nm. A drastic change in the curve occurs between 1500 and 1700 nm penetration depth and is followed by a significant increase in derivative value until the final load of 50 mN is achieved. Event presence was consistent for all analyzed curves but did not occur at the same displacement locations or have the same shape. The derivative value always continued to increase after the event. This behavior might be due to either or a combination of substrate effects, delamination of the film, or cracking. No events are found in the unloading portion of the curve, suggesting a normal elastic response.

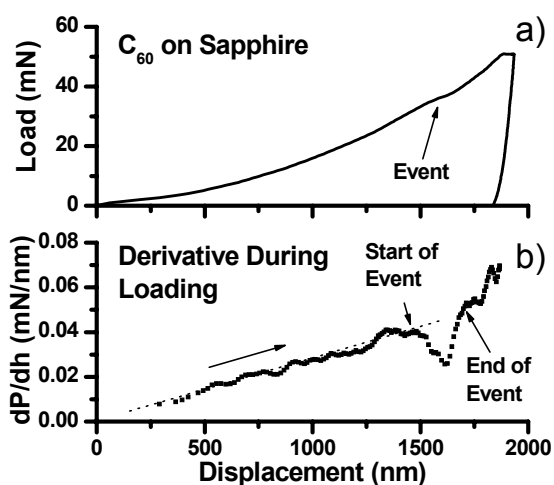


**Figure 3:** *C*<sub>60</sub> on sapphire load-displacement curve (a) and the derivative behavior of the loading curve (b). The dashed line shows a linear fit.

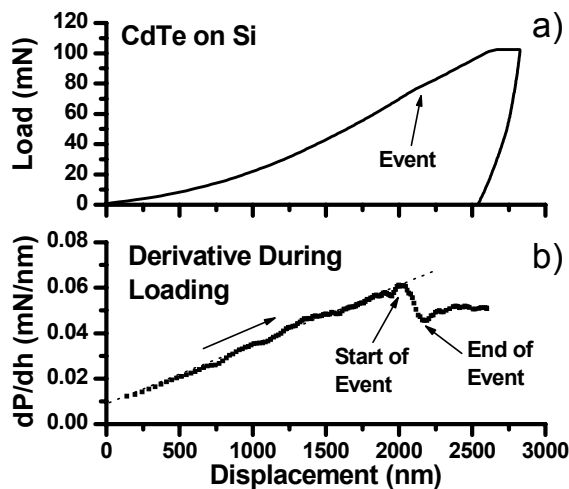


**Figure 4:** *CdTe* on *Si* load-displacement curve (a) and the derivative behavior (b) of the loading curve. The dashed line shows a linear fit.

Fig. 4 illustrates a result from the second material system studied, a CdTe thin film on single-crystal silicon (Table 1). A load-displacement curve is given in Fig. 4(a) and the resultant derivative behavior is given in Figs. 4(b) and 4(c). The load-displacement curve does not clearly show a transient event. However, in the derivative behavior, the precise location of onset and termination of the event is observed near 2000 nm (Fig. 4(b)), at about 15% of the film's thickness. It is seen that the derivative of the load-displacement curve decreases after the event, signifying that it is not due to a harder substrate effect. Therefore, this change might be due to film delamination or cracking. Furthermore, this event was consistently not seen for indents that had a maximum load of only 50 mN.

### III. Kink Pop-Out

“Kink pop-out” is a term attached to a transient event during unloading that appears as a cubic shape or a kink, and is observed in single-crystal silicon load-displacement curves [16,17]. It is thought to be caused by indentation-induced phase transformation and cracking as the material physically pops out [16]. Fig. 5 illustrates the appearance of a kink pop-out event in the load-displacement curve (Fig. 5(a)) and in the derivative behavior (Fig. 5(b)). It is evident within a 25 nm range where the kink shape (event) begins in the load-displacement curve, but is clear to within a 5 nm range in the derivative plot. This event has been shown by Raman microspectroscopy to correspond to the nucleation of r8 structured Si-XII from metallic  $\beta$ -tin structured Si-II that exists underneath the tool [16], with the transformation complete at the end of the event.

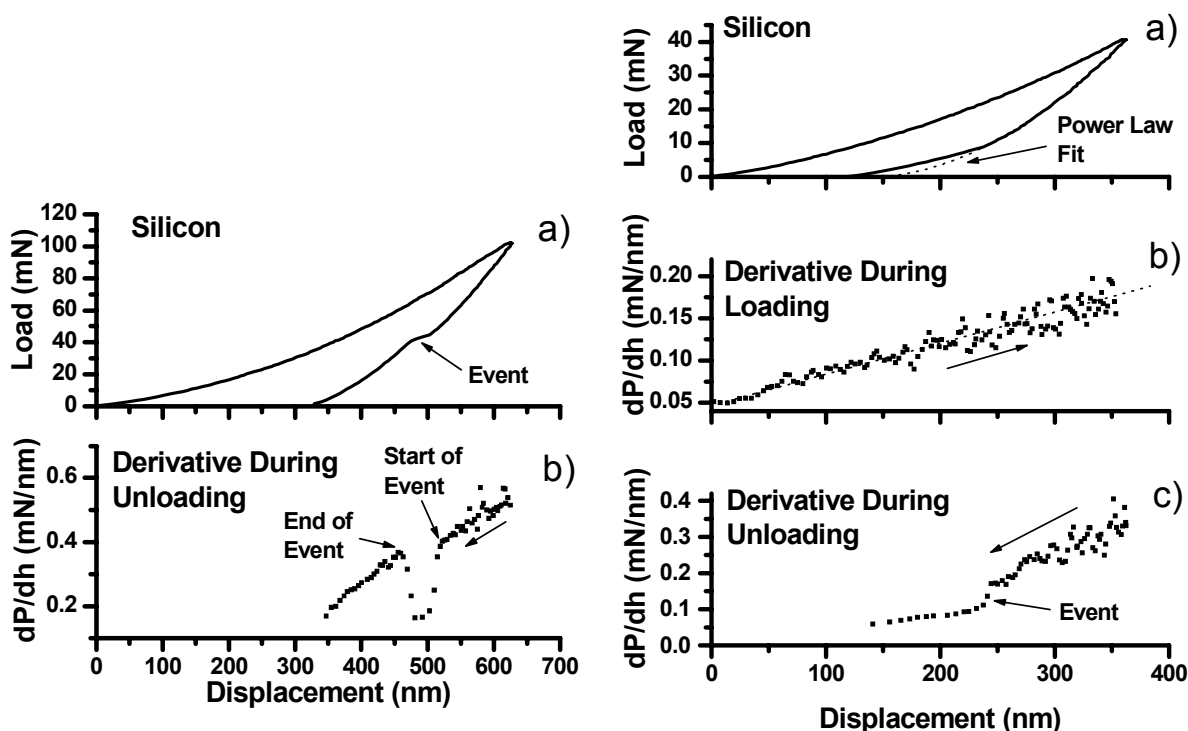


**Figure 5:** Silicon load-displacement curve (a) and derivative behavior (b) for a kink pop-out event.

**Figure 6:** Silicon elbow load-displacement curve along with power-law fit (dashed line) (a), derivative behavior on loading (b) and unloading (c) for the elbowing event. The dashed line in (b) shows a linear fit.

#### IV. Elbowing Behavior

Broadly defined, elbowing behavior is an accelerated slope decrease in the unloading curve, such that Eq. (3) can no longer describe the unloading load-displacement response. During unloading, elbowing behavior will always display smooth upward concavity in its derivative response. Two materials studied exhibited such behavior. A resultant curve for elbowing in silicon is shown in Fig. 6(a). For silicon, elbowing behavior can be induced with a sharp indenter by quickly unloading the material from a maximum applied load of about 10-60 mN [16]. It is thought to be due to the transformation of Si-II to amorphous silicon [6]. Derivative behavior during loading (Fig. 6(b)) shows that although noisy, silicon displays a regular loading curve that may be approximated by a linear fit. During unloading (Fig. 6(c)), there is a sudden drop in  $dP/dh$  at the onset of the elbowing behavior, signifying the start of amorphous silicon formation under the indenter tip. Analyzing different silicon curves with elbowing behavior showed different magnitudes for this drop, but the feature was always present. After this drop, derivative behavior begins to stabilize. In Fig. 6(a), a power-law curve fit comparison is alongside the experimental curve, using the upper 50% of the unloading curve for the fit. The power-law fit begins to deviate from the experimental curve at a similar point where the drop occurs, although the fitting method itself can be a somewhat ambiguous procedure.

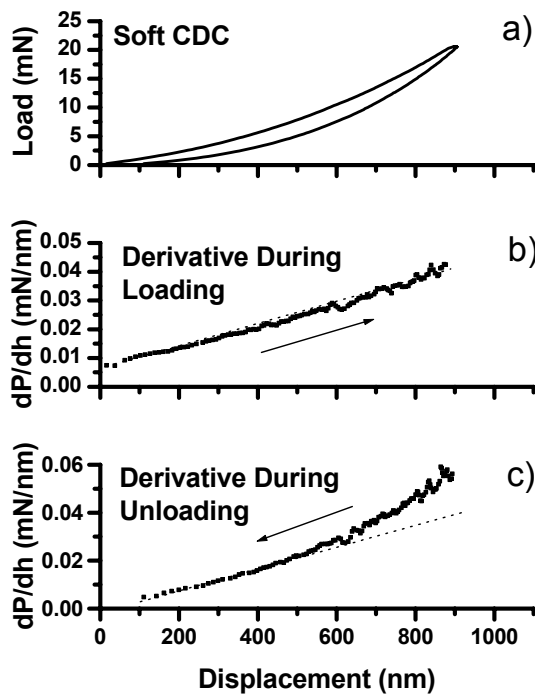


**Figure 7:** Soft CDC load-displacement curve (a) and derivative behavior on loading (b) and unloading (c) for the elbowing event. The dashed lines in (b) and (c) show a linear fit.

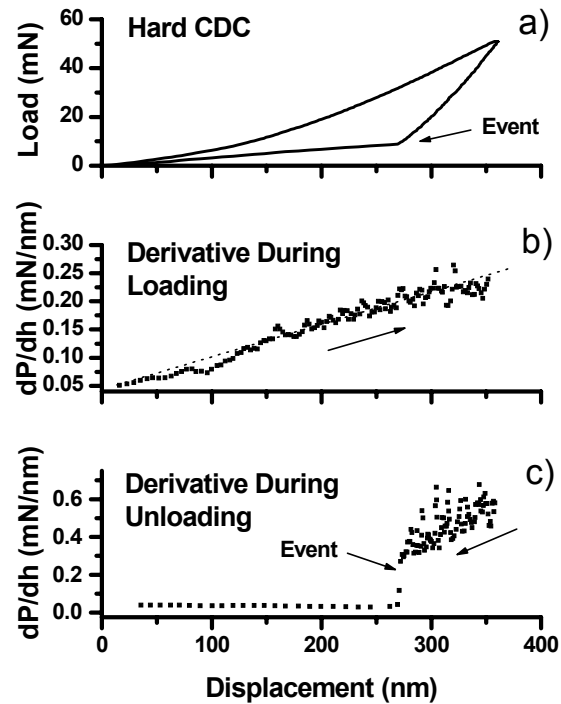


**Figure 8:** Load-displacement curve (a), first derivative behavior during loading (b) and unloading (c) for hard CDC.

The other material studied that consistently exhibited elbowing behavior was soft CDC, a material whose synthesis methods are reported elsewhere, but which is essentially comprised of nano-porous nano-crystalline carbon [18]. The reasons for the elbowing behavior in CDC (Fig. 7) are not understood at this time. This material exhibits a normal loading response (Fig. 7(b)) that is indicative of fitting Eq. (1). Upon unloading, smooth upward concavity can be observed. The upper 50% of the unloading curve could not be successfully fit to Eq. (3) suggesting that elbowing behavior begins at an earlier stage than silicon. Like the silicon elbow derivative curve, after a certain point (in this case around 600 nm depth) the data begins to be smooth. However, there is no sudden event before this point so the derivative method provides only the fact that elbowing behavior is occurring.

## V. Sharp Unloading Curve Bending

Two materials were tested that sometimes exhibited sudden, sharp bends in their unloading curves; hard CDC coatings and a 50% PMMA/HA particle composite created for biomedical applications. Load-displacement and derivative behavior for a selected CDC coating indent can be seen in Fig. 8. Although it is clear from the load-displacement curve (Fig. 8(a)) where the unloading event begins, derivative behavior during loading (Fig. 8(b)) and unloading (Fig. 8(c))

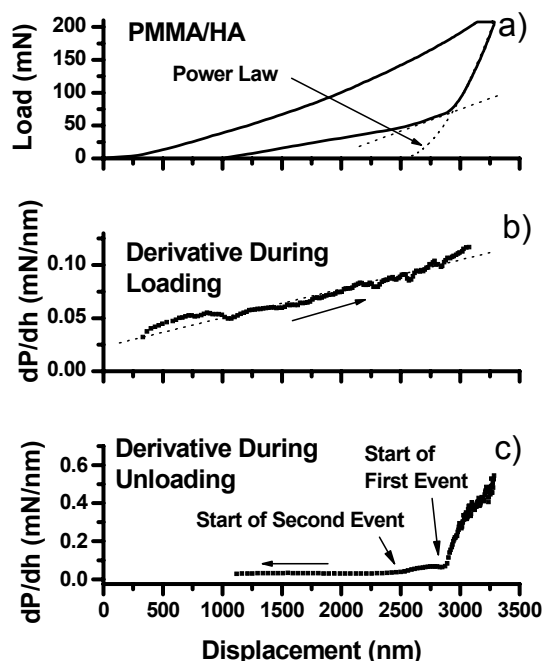


**Figure 9:** Load-displacement curve along with power-law fit (a), derivative behavior on loading (b) and unloading (c) for a PMMA/HA particle composite. The flat line in (a) is to illustrate the second out of three portions of the unloading curve.

is reported to illustrate its behavior in such an instance. A key feature that separates a sharp unloading curve bending response from the elbowing response is that the derivative response effectively becomes flat after the sharp bend. Similar behavior was also observed for a PMMA/HA particle reinforced composite. HA has a reported hardness and modulus of 6.5 GPa and 125 GPa, respectively [19], and PMMA was tested to have a hardness in the MPa range and a modulus of about 1 GPa (Table 1). Behavior for the PMMA/HA particle matrix can be seen in Fig. 9. From scrutinizing the load-displacement curve in Fig. 9(a), it can be seen that there are at least two distinct changes and three independent segments occurring during unloading. Looking at the derivative behavior during unloading (Fig. 9(c)), the beginning of each segment can be seen.

The cause of such events during unloading are not well understood at this time, but most likely occur for one or a combination of two reasons. The first reason is that the indenter tool is laterally displaced because it encounters significant local roughness during loading. Derivative behavior upon loading in both hard CDC (Fig. 8(b)) and PMMA/HA (Fig. 9(b)) is found to contain transient events near the beginning of the loading segment, suggesting that inhomogeneous surface conditions exist underneath the tool. Upon unloading, it then begins to laterally move back into its original place, starting at the point where the sharp bend in the curve is. The second reason is that the material is undergoing some sort of phase transformation under the tool during loading, dynamically changing conditions, and an accelerated recovery of the material occurs upon unloading.

## GENERAL CONSIDERATIONS AND COMMENTS

For quantification purposes, applications of this method are numerous. The point where substrate properties, film delamination, or cracking begin for thin films can be found, so that experimentally one knows how deep they can indent a thin film to get reliable properties. Upon unloading, contact pressures at the beginning of events may be found with the methods described in Reference 16. If an event occurs and eventually recovers, as in the case of the kink pop-out, the event duration may be determined. As a final example, using power-law curve fitting of the upper unloading portion and extrapolating, an estimation of the material recovery due to an event may be found.

These methods might also prove useful with spherical or conical indenter tips, but the derivative features may be different because of the strain gradients involved in the area immediately below the tool. For example, crack densities and propagations are different for Berkovich and spherical tools and should yield different event locations or derivative shapes. Furthermore, Hertzian elastic contact loading for a spherical tool is known to be able to be described as

$$P = Ch^{3/2} \quad (6)$$

where  $C$  is a material and indenter tip related constant. Therefore, this method might not be as useful for elastic or spherical loading events because the magnitude of deviation from linear behavior would be more difficult to detect. Methods computing  $dP/dh^{1/2}$  instead might be more suitable. This is also the case for the spherical part of a conical indenter. However, the current  $dP/dh$  method should work excellently for other sharp self-similar indenter tip shapes such as Vickers and cube corner.

One should have the most stable environment possible to run these tests, and the data collection rate should be set to the highest possible values. Some depth-sensing indentation machines can collect data points at 2000 Hz or higher. Increasing data collection rate will improve the accuracy for which event locations can be detected.

## CONCLUSIONS

It has been shown for several materials that numerical first derivative analysis can be very useful to determine the presence and place of onset for transient events that may occur for a number of reasons. The load-displacement and derivative behavior for transient events on loading, kink pop-out, elbowing, and sharp unloading curve bending were presented. In most cases, using only the first derivative is good enough to see the location of event onsets. Noting the concavity of resultant derivative plots aids in deciphering the type of behavior present. A major strength of this method is that its success is not dependent on knowing accurate tip area coefficients or specific material properties. Also, the derivative behavior can be easily calculated via a spreadsheet within minutes, making this a quick method to employ for routine load-displacement curve analysis.

## ACKNOWLEDGEMENTS

T.J. was supported to do this work by a National Defense Science and Engineering Graduate fellowship. Much thanks is given to Ms. E. Ho for the PMMA/HA sample and to Mr. D. Ge for his useful input into this paper, both at Drexel University. Thanks is given to Mr. J. Jungk at the University of Minnesota for his ideas contributing to this paper. This work was funded by the National Science Foundation (NSF) through grant number DMR-0196424.

## REFERENCES

1. W. C. Oliver and G. M. Pharr, *J. Mater. Res.* **7**, 1564 (1992).
2. R. Saha and W. D. Nix, *Acta Mater.* **50**, 23 (2002).
3. R. Nowak, T. Sekino, and K. Niihara, *Acta Mater.* **47**, 4329 (1999).
4. E. R. Weppelmann, J. S. Field, and M. V. Swain, *J. Mater. Res.* **8**, 830 (1993).
5. J. E. Bradby, J. S. Williams, J. Wong-Leung, et al., *Appl. Phys. Lett.* **77**, 3749 (2000).
6. V. Domnich, Y. Gogotsi, and S. Dub, *Appl. Phys. Lett.* **76**, 2214 (2000).
7. Y. G. Gogotsi, V. Domnich, S. N. Dub, et al., *J. Mater. Res.* **15**, 871 (2000).
8. S. V. Hainsworth, H. W. Chandler, and T. F. Page, *J. Mater. Res.* **11**, 1987 (1996).
9. M. Sakai, S. Shimizu, and T. Ishikawa, *J. Mater. Res.* **14**, 1471 (1999).
10. J. Malzbender and G. de With, *Surf. and Coatings Tech.* **127**, 266 (2000).
11. M. R. McGurk and T. F. Page, *J. Mater. Res.* **14**, 2283 (1999).
12. S. V. Hainsworth, M. R. McGurk, and T. F. Page, *Surf. and Coatings Tech.* **102**, 97 (1998).
13. J. Malzbender and G. de With, *Surf. and Coating Tech.* **137**, 72 (2001).
14. G. M. Pharr and A. Bolshakov, *J. Mater. Res.* **17**, 2660 (2002).
15. A. Richter, R. Ries, R. Smith, et al., *Diamond and Related Mat.* **9**, 170 (2000).
16. T. Juliano, Y. Gogotsi, and V. Domnich, *J. Mater. Res.* **18**, 1192 (2003).
17. V. Domnich and Y. Gogotsi, *Rev. Adv. Mater. Sci.* **3**, 1 (2002).
18. Y. Gogotsi, S. Welz, D. Ersoy, et al., *Nature* **411**, 283 (2001).
19. R. Kumar and M. Wang, *Mat. Sci. and Eng. A* **338**, 230 (2002).